**ORIGINAL PAPER**

# Fire-Resistant Bio-based Polyurethane Foams Designed with Two By-Products Derived from Sugarcane Fermentation Process

Ana Paula Capêto[1] · Manuela Amorim[1] · Sérgio Sousa[1] · Joana R. Costa[1] · Braian Uribe[2] · Ana Sofia Guimarães[3] · Manuela Pintado[1] · Ana L. S. Oliveira[1]

## Abstract

There is a growing interest in replacing conventional fossil-based polymers and composites with waste-based materials and fillers for environmental sustainability. This study designed water-blown polyurethane rigid foams using two by-products from the Amyris fermentation process of producing β-farnesene. The distillation residue (FDR) served as the main polyol component in the foam's formulation (PF), supplemented with 4.5% sugarcane bagasse ash (SCBA) as a fire-retardant filler (PFA). The study assessed the impact on foam properties. Based on the analysis of all compiled data (foam structure, mechanical, and thermal properties), it can be inferred that ash particles acted as nucleating points in the reaction media, leading to a reduction in foam density (from 134 to 105 kg/m$^3$), cell size (from 496 to 480 nm), and thermal conductivity. The absence of chemical interaction between the ash filler and the polyurethane matrix indicates that the ash acts as a filler with a plasticizing effect, enhancing the polymer chain mobility. As a result, the glass transition temperature of the foam decreases (from 74 to 71.8 ℃), and the decomposition onset temperature is delayed. Although, the incorporation of 4.5% SCBA (grain size below 250 μm) was ineffective in the increment of the compressive strength, that small amount was enough to increase the foam's specific strength from 1009 to 1149 m$^2$/s$^2$ suggesting that other factors (e.g. polyol feedstock, grain size, ash packing, etc.) are yet to be accounted. The flammability test results indicate that sugarcane bagasse ash improved the foam performance, reducing burning time from 251 to 90 s, time of extinguishment from 255 to 116 s, and burning length from 132 to 56.7 mm, meeting the fire protection standard UL 94, class HB. Despite the need for further improvement and detailed flammability evaluation, the results support the notion that polyurethane foams from renewable waste by-products offer a sustainable alternative to both edible and fossil-based sources. Additionally, sugarcane bagasse ash can be a suitable silica source for reinforcing composites with reduced flammability, potentially replacing harmful halogenated chemicals used for the same purpose.

✉ Ana L. S. Oliveira
asoliveira@ucp.pt

1    Centro de Biotecnologia e Química Fina (CBQF), Laboratório Associado, Escola Superior de Biotecnologia, Universidade Católica Portuguesa, Rua Diogo de Botelho 1327, 4169-005 Porto, Portugal

2    Departamento de Engenharia de Polímeros, Instituto de Polímeros e Compósitos, Universidade do Minho, Campus de Azurém, 4800-058 Guimarães, Portugal

3    CONSTRUCT, Faculdade de Engenharia do Porto (FEUP), Universidade do Porto, Rua Doutor Roberto Frias, 4200-465 Porto, Portugal

**Graphical Abstract**
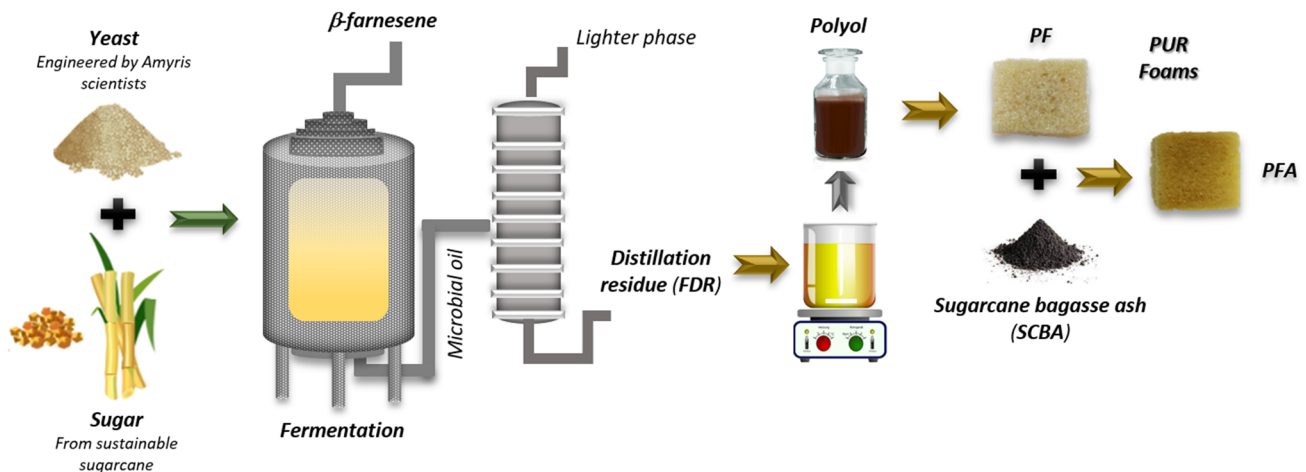


**Keywords** Sugarcane bagasse ash · Microbial oil · Polyurethane foam · Fire-resistant · Bio-based

## Introduction

The circular economy is already recognized as a regenerative system model that endorses the efficient use of resources through waste minimization, long-term value retention, reduction of primary resources, and closed loops of materials within the boundaries of environmental protection and socio-economic benefits [1].

The increasing awareness of petroleum reserves depletion [2, 3], together with subsequent floating prices triggered the implementation of sustainable technologies to reduce the environmental impact and minimize the footprint of fossil-based plastics replacing them with bio-based materials [4].

Polyurethane foams are usually the product of a polymerization reaction between an isocyanate (e.g., methyl diphenyl diisocyanate, MDI) and a fossil-based polyol, blended using customized formulations that depends on the final application and generally involve the use of catalysts, surfactants, blowing agents, chain extenders, etc. [5, 6]. That reaction results in a cellular structure characterized by resistance to water exposure, relevant mechanical properties, and low thermal conductivity coefficients, enabling their application, for example, in furniture, bedding, and thermal-insulating systems, such as refrigerating units, pipe and roof insulation and wall padding for building purposes [7–9].

In the last decades, the need to replace non-renewable feedstock led to the synthesis of bio-based polyols using a range of natural renewable resources has been the subject of expanded research [10, 11]. The feedstock ranges from edible oils (e.g. soybean, sesame, and sunflower oils), to biomass lignocellulosic residues and non-edible vegetable oils which don't compete with the food industry, such as castor, jatropha, and neem oils, etc. [12]. Other oily wastes are also subject of many studies, for example, waste cooking oil [13], fish oil [14], and microbial oils [15, 16].

The chemical composition, low density and air permeability of polyurethane foams promotes flammability, enhancing fire expansion [17]. To counteract this effect, and to reduce combustibility and suppress toxic fumes or smoke production, flame retardants have been used, e.g., inorganic fillers, organic phosphorous compounds, nitrogen-based materials, and halogenated materials [17, 18]. Biomass ash derived from industrial by-products such as rice husk or sugarcane bagasse, is a natural and suitable eco-friendly waste material with a high content in silica, which is known to act as flame retardant, improving thermal stability and mechanical properties in polyurethane foams [19–21]. Recently a research study revealed that the incorporation of 50% of waste ash improved heat release by 69% and reduced $CO_2$ and $CO$ emissions by 76 and 77%, respectively, during a fire [22].

Amyris patented brand molecule called trans-ß-farnesene is synthesized using conventional fermentation of sugar syrup from sugarcane by genetically modified *Saccharomyces cerevisiae* [23, 24]. This process generates a distillation residue, a microbial oil composed by a certain amount of wax esters (0.22% wt), hydrocarbons (43.29%), a small percentage of complex lipids such as tri- and di-glycerides along with farnesol, terpenes such as β-farnesene, sesquiterpenes, and triterpenes [25]. The chemical profile akin to vegetable oils and the iodine value around 130 g $I_2$/100 g [26] indicates a certain degree of unsaturation and the possibility to synthesize polyols for condensation polymers,

exemplified by the polyurethane class, which implies a set of chemical reactions to achieve the necessary functionalization that explores carbon–carbon double bonds and ester linkages present in natural oils [27–29].

The main purpose of this manuscript was to use this microbial oil residue to produce a polyol that will represent the polyurethane backbone in a formulation supplemented with sugarcane bagasse ash, as a flame-retardant additive. The properties of the formulated bio-based polyurethane foams will be discussed.

## Materials and Methods

### Materials and Reagents

B-farnesene distillation residue (FDR), (iodine number of 122 g $I_2$/100 g) was provided by Amyris Inc. (Campinas, Brazil) and characterized elsewhere [25].

Sugarcane bagasse ash (SCBA) was provided by Raízen/Amyris (Brazil). Both materials were transported from Brazil to the CBQF-UCP laboratory (Porto, Portugal) under refrigerated conditions.

Ethyl acetate and glycerol (99%) were supplied by Carlo Erba (Milan, Italy) and formic acid (98%) by Fluka™ Honeywell (New Jersey, United States). Ethanol (96%), hydrogen peroxide ($H_2O_2$, 35%) and monohydrated sodium hydrogen carbonate ($NaHCO_3$) were purchased from Labchem (Pennsylvania, United States). Sigma–Aldrich (St. Louis, United States) supplied all the analytical grade reagents such as 1-butanol, 4-diphenylmethane diisocyanate (4,4-MDI), acetic anhydride, dibutyltin dilaurate (DBTDL), hydrofluoric acid (HF 40%), nitric acid ($HNO_3$ 65%), phenolphthalein indicator, phosphoric acid (H3PO4, 85%), poly(dimethyl siloxane) (PDMS), potassium hydroxide (KOH) standard solution (Titrisol®), pyridine (99%), and HPLC grade tetrahydrofuran.

**Table 1** FDR-based water-blown PUR foam composition, neat foam (PF) and ash-reinforced (PFA)

| Sample | Role | Amount (wt%) | |
|---|---|---|---|
| | | PF | PFA |
| FDR-based polyol | Monomer | 17.7 | 16.9 |
| Water | Blowing agent | 1.2 | 1.2 |
| Glycerol | Chain-extender | 19.0 | 18.1 |
| DBTDL | Catalyst | 0.8 | 0.8 |
| PDMS | Emulsifier | 2.8 | 2.7 |
| 4,4'-MDI | Monomer | 58.5 | 55.8 |
| SCBA | Fire-retardant | – | 4.5 |

## Procedure

*Pretreatment of the filler* Sugarcane bagasse ash (SCBA) was subjected to a thermochemical pretreatment mainly to oxidize the organic matter present in the received samples. The ash was loaded in a porcelain crucible placed in a laboratory muffle and heated from room temperature to 600 °C at a rate of 10 °C $min^{-1}$, followed by a stage at 600 °C for 5 h. After cooling to room temperature, 1.0 mL of hydrogen peroxide was mixed in a crucible with about 15 g of ash and proceeded to another 600 °C heating cycle.

*Polyol synthesis* was carried out by a simple two-step mechanism of FDR epoxidation with performic acid formed in situ according to the method described in Uprety et al. [15], followed by oxirane ring-opening using the acid-hydrolysis route [15, 30]. This technique is commonly used to insert hydroxyl groups in the structure exploring carbon–carbon double bonds and ester linkages present in natural oils [31].

FDR (200 g), ethyl acetate (100 g), and formic acid (12 g) were weighed in a closed borosilicate vessel with a three-way lid and placed on a heating/stirring plate (Hei-Tech, Heidolph Instruments GmbH & Co.KG, Schwabach, Germany). After a few minutes of constant stirring, refrigerated hydrogen peroxide (320 g) was slowly poured to avoid exothermic foaming. The epoxidation took place at 65 °C for 6 h with constant stirring, followed by decantation of the organic phase in a separatory funnel and a neutralization/washing operation with water and sodium bicarbonate solution (10%). The epoxide was then dried overnight at 80 °C in a vacuum oven (Binder, model VD23).

In the next step, epoxide (EBT) and phosphoric acid ($H_3PO_4$) (ratio 7:1 wt.) were loaded in the vessel and heated until 85 °C for 1 h. The neutralization/purification operation was conducted in the same way. Under these conditions ($H_3PO_4 = 12.5\%$, with total phosphorus content = 4%) formation of a phosphate-polyol containing mono-, di-, and tri- phosphate esters [30, 32] is expected.

The reaction yield ($\eta$) was determined by Eq. (1).

$$\eta\,(wt\%) = \frac{m_{polyol}(g)}{m_{FDR}(g)} \times 100 \tag{1}$$

where, $m_{FDR}$ was defined as the mass of the feedstock used to polyol synthesis (FDR, 200 g), and $m_{polyol}$ mass of polyol produced.

*Polyurethane foams preparation* Two formulations (Table 1) were developed for both bio-based polyurethane foams with ash (PFA) and without ash (PF). Water was used as a green reagent to react during the polymer network formation by in situ generation of the blowing agent carbon dioxide ($CO_2$) [33]. In the first stage all ingredients, with exception of 4,4-MDI, were weighed into a beaker and

melted, in a hotplate while mechanically mixed for 2 min. In the second stage, the pre-measured MDI was added, and the content was manually stirred for 8–20 s. The free-rising foam was left to cure and stabilize for 48 h at room temperature [34].

## Materials Characterization

### Pre-treated Sugarcane Bagasse ash (SCBA)

*Apparent bulk density ($\rho_{SCBA}$)* was determined following the method ASTM D7481-18 [35] guidelines. The ash was loosely poured through a funnel of adequate aperture into a graduated cylinder that was tapped to accommodate the particles in the confined space. The apparent density was determined by Eq. (2) as the ratio between the weight of the material ($m_{ash}$) in the cylinder by the respective volume ($V_{ash}$). The result expressed in kg/m$^3$, represent the mean value obtained from three independent measurements.

$$\rho_{SCBA}(kg/m^3) = \frac{m_{ash}}{V_{ash}} \tag{2}$$

*Particle size diameter (dp)* was evaluated following the ASTM C136/ C136M-19 [36] standard method general guidelines. The treated ash was poured through a stack of sieves (500, 375, 250, and 100 μm), mounted in an analytical sieve shaker system (model AS 200, Retsch GmbH, Haan, Germany) for 20 min and vibration amplitude of 3 mm.

*Quantification of minerals* was performed by Inductively Coupled Plasma—Atomic Emission Spectrometry (ICP-AES). Briefly, 250 mg of the oxidized ash was mixed in a Teflon vessel with 2 mL of $HNO_3$ and 2 mL of HF and heated in a microwave system (Berghof, Eningen, Germany). The digestion procedure was conducted in four steps: 140 °C and 40 bar for 5 min; 160 °C and 40 bar for 10 min; 200 °C and 40 bar for 30 min; 100 °C and 20 bar for 5 min. After microwave digestion, the samples were cooled down to room temperature and diluted to a final volume of 50 mL. Microwave-digested samples were then analyzed through ICP-AES (PerkinElmer, Massachusetts, USA) and quantified through external standard calibration. All analyses were performed in triplicate.

### Polyol Characterization

*Acid value* was determined by titrimetric analysis following ASTM D4662-20 [37] and corresponds to the amount of carboxylic acid groups present in the sample expressed in mg of potassium hydroxide (KOH) per g sample i.e. mg KOH/g. In a 250 mL Erlenmeyer flask, a known quantity of polyol (weighed to the nearest 0.1 mg) was thoroughly dissolved in 50 mL of solvent mixture (toluene: ethanol, ratio 1:1 v/v). The sample free acids were titrated against a standard ethanolic solution of potassium hydroxide (KOH, 0.1 N) in the presence of 0.5 mL of phenolphthalein indicator. A blank determination was carried out with 50 mL of the titration solvent. The analysis was performed in triplicate and the average acid value was calculated by the equation (3)

$$Acid\ Value\ (mg_{KOH}/g) = \frac{(V_s \times N \times 56.1)}{W_s} \tag{3}$$

where: $V_s$ = volume of KOH ethanolic solution required for titration of the sample, mL, $N$ = normality of the KOH ethanolic solution, 56.1 = $KOH$ molecular weight, $W_s$ = sample weight, g.

*Hydroxyl (–OH) value* was determined by titrimetric analysis following ASTM E222-17 Test Method B (Reflux Method) [38]. This analytical method involved the acetylation of primary and secondary hydroxyl (–OH) groups with acetic anhydride in pyridine under reflux conditions. After reaction completion, distilled water and 1-butanol were added and the remaining unreacted acetic anhydride was converted to acetic acid and measured by titration with 0.5 N potassium hydroxide (KOH) standard solution in the presence of phenolphthalein indicator. The analysis was performed in triplicate, and the average hydroxyl (–OH) value expressed as milligrams of potassium hydroxide equivalent to the hydroxyl content of 1 g of the polyol was determined by the Eq. (4).

$$Hydroxyl\ value\ (mg_{KOH}/g) = \frac{(V_b - V_s) \times N \times 56.1}{W_s} + Acid\ Value \tag{4}$$

where: $V_b$ = volume of $KOH$ solution required for titration of the reagent blank, mL, $V_s$ = volume of KOH solution required for titration of the acetylated specimen, mL, $N$ = normality of the KOH solution, $W_s$ = weight of the sample used for acetylation, g, and the value 56.1 = KOH molecular weight, g/mol.

*Dynamic Viscosity* was measured in triplicate at 25.0 °C, following the standard ASTM D4878-15 Test Method A [39] guidelines that determine the viscosity of polyols in the range 10–100,000 mPa.s, using a rotational viscometer from Rheology Instruments, (model B-One Plus, Lamy Rheology Instruments, Champagne au Mont d'Or, France).

*Molecular weight ($M_w$) distribution* was determined by high-performance liquid chromatography (HPLC). The chromatograms were acquired using an HPLC (model 1260 Infinity II, Agilent Technologies, Santa Clara, CA, USA) attached to an Evaporative Light Scattering Detector (ELSD,

1290 Infinity II, Agilent Technologies, Santa Clara, CA, USA) with evaporation temperature at 70 °C and nebulization at 65 °C, using nitrogen as nebulizing gas coupled to a TSK gel GMHxL column for insoluble polymers. The isocratic analysis was carried out with tetrahydrofuran as the mobile phase; flow rate of 0.6 mL min$^{-1}$; sample concentrations of 20–25 mg mL$^{-1}$ dissolved in THF and injection volumes of 20 µL. The molecular weight was estimated by calibration curve of polystyrene standards 400–303.000 Da (Agilent (Waldbronn, Germany).

*Equivalent weight (E)* based on the hydroxyl value (–OH) was calculated using Eq. (5).

$$E = \frac{1000 \times 56.1}{[-OH]} \tag{5}$$

*Functionality (f)* was calculated as the ration of the average molecular weight ($M_w$) and equivalent weight (E) as defined by Eq. (6).

$$f = \frac{M_w}{E} \tag{6}$$

## Polyurethane Foams

*Apparent density ($\rho_{foam}$)* was determined following ASTM D1622/D1622M-14 methodology for rigid cellular plastics. Test specimens with average dimensions ($4.5 \times 5.0 \times 1.0$) cm were cut, measured by a caliper (precision 0.1 mm) and weighed on a balance (precision 0.1 mg). The foam apparent density determined by Eq. (7) was calculated as the ratio of the sample weight to its volume. The results expressed in kg/m$^3$, represent the mean values obtained from six independent measurements.

$$\rho_{foam}\left(kg/m^3\right) = \frac{mf}{Vf} \tag{7}$$

*Compressive strength* was determined following the ASTM D1621-00 guidelines. The test samples were cut into cubes, and the experiment was carried out at room temperature and humidity using a heavy-duty platform (HDP/90) with a 5 mm stainless steel cylindrical probe (P/0.5R) with a 30 kg load cell attached to a TA.XT 2i Texture Analyzer (Stable Micro Systems, Godalming, U.K.). The compression force was applied in the foam rise direction, with a pretest speed was set at 1 mm/s, the test speed was 1.70 mm/s, and the post-test speed was 10 mm/s. The compressive strength ($\sigma$) as indicated by Eq. (8), was calculated by the ratio between the value of the maximum force (F) applied to a sample with initial cross-sectional area (A) when the maximum applied force occurred approximately at 10% of

deflection. The results, expressed in kPa represent the mean values obtained from three independent measurements.

$$\sigma(kPa) = \frac{F}{A} \tag{8}$$

The *specific strength* was determined by Eq. (9) as the ratio between the compressive strength ($\sigma$) and the apparent density ($\rho_{foam}$) and is expressed in m$^2$/s$^2$.

$$Specific\ strength\ \left(m^2/s^2\right) = \frac{\sigma}{\rho_{foam}} \tag{9}$$

*Thermal properties* were determined by differential scanning calorimetry (DSC) analyses were carried out using a NETZSCH DSC204 calorimeter. Nitrogen was used as the purge gas at 40 mL/min. Approximately 2 mg of each sample was placed in aluminum pans and the thermal properties were recorded between − 50 and 200 °C at 10 °C·min$^{-1}$ to observe the glass transition temperature. The glass transition temperatures ($T_g$) were measured on the second heating ramp to erase the thermal history of the polymer.

*Thermal conductivity* was determined following EN 10456 guidelines using a thermal analyzer (Isomet 2114, Applied Precision) with a surface probe (IPS 1105) and a calibration standard (XPS, IBER Fibran). The samples dimensions were 100 mm × 100 mm × 40 mm, and the results, expressed in W.m$^{-1}$.K$^{-1}$are the mean values calculated from three independent measurements.

*Morphology analysis* was performed by Scanning Electron Microscopy (SEM) using a JSM-5600LV (JEOL; Tokyo, Japan). Samples with 3 mm × 5 mm sliced with a scalpel from the center of the foam were placed directly on top of double-sided adhesive carbon tape (NEM tape, Nisshin, Japan), covering metallic stubs, and coated with gold/palladium using a sputter coater (Polaron, Bad Schwalbach Germany). All observations were performed using the secondary electron (SE) detector, with the SEM operated in high-vacuum, at an acceleration voltage of 15 kV and a spot size of 20. The average pore diameters were determined using ImageJ 1.53e software (USA).

*Flammability test* of rigid polyurethane was performed following the ASTM UL 94 HB standard for safety. This standard describes a set of a small-scale reaction test methods covering the flammability of new polymeric materials used for parts in devices and appliances and they are intended to serve as a preliminary indication of their acceptability with respect to flammability for a particular application. In this test a standard test specimen of 50 (W) × 150 (L) × 13 (H) mm of both polyurethane foams was exposed to a horizontal flame for 10 s, forcing its ignition. After that period of time the flame was

**Table 2** Sugarcane bagasse ash (SCBA) mineral composition

| Compound | Concentration (g/100 g) |
|---|---|
| $SiO_2$ | $59.5 \pm 3.1$ |
| $Fe_2O_3$ | $17.8 \pm 0.0$ |
| $K_2O$ | $2.5 \pm 0.0$ |
| CaO | $2.2 \pm 0.2$ |
| $P_2O_5$ | $1.3 \pm 0.1$ |
| $Al_2O_3$ | $0.9 \pm 0.1$ |
| MgO | $0.9 \pm 0.0$ |
| Na | $0.2 \pm 0.0$ |
| $MnO_2$ | $0.1 \pm 0.0$ |

extinguished, and the samples free burning characteristics were observed.

*Attenuated Reflectance Fourier Transform Infrared Spectroscopy* (ATR-FTIR) was used to envision the chemical structure of all materials (FDR, epoxide, polyol, and foams) in the near-infrared range. Analyses were conducted in the absorbance range of 4000 to 500 cm$^{-1}$, using a Perkin Elmer FT-IR spectrophotometer, fitted with a Pike Miracle ATR accessory containing Zn/Se crystal.

## Statistical Analysis

The results were displayed as the mean $\pm$ standard deviation (n = 3). The Shapiro–Wilk test was employed to assess the normality of data distribution, and the null hypothesis of equal means was rejected if the difference between means was $p < 0.05$. After conducting the ANOVA, multiple comparisons were performed on statistically significant variables using Tukey's post-hoc test, assuming homogeneity of variance at the $p < 0.05$ significance level. All statistical analyses were conducted using STATISTICA version 14.0.0.15 (TIBCO Software Inc.).

**Table 3** Polyol characterization

| Measured property | Units | FDR-based polyol |
|---|---|---|
| Acid value | mg KOH/g | $3.3 \pm 1.0$ |
| Hydroxyl (–OH) value | mg KOH/g | $82.3 \pm 0.9$ |
| Viscosity at 25 °C | mPa.s | 13,256 |
| Molecular weight | Da | $2711.3 \pm 10.0$ |
| Functionality (f) | – | $4.0 \pm 0.1$ |
| Yield | % | $80.3 \pm 11.4$ |

## Results and Discussion

### SCBA Characterization

A vast quantity of sugarcane bagasse ashes are daily produced in cogeneration plants, and though already used as filling materials in the construction industry [40, 41] they are commonly placed on soil for fertilizing purposes or simply dumped in ponds and landfills, leading to great environmental concerns [42, 43].

In the polymer industry, natural alternatives with silica content have been used, as inorganic fillers obtained from recycling residues to reinforce polymers composites [44]. The char layer formed by a inorganic filler is a natural mass transfer barrier that improves the burning resistance of polymers, delaying the release of volatile compounds and improving insulation properties [45].

The ash used in this study was supplied by Raízen cogeneration plants and presented an irregular and rough texture containing fine burnt and coarse unburnt particles. According to characterization performed in previous studies [46, 47] those ashes after removal of the particle size fraction above 500 µm, presented an apparent density around 2330 kg/m$^3$, 5% of moisture content, 82% of minerals, and 12% of organic matter.

The thermo-chemical treatment with a strong oxidizing agent (hydrogen peroxide) and high temperatures (600 °C), allowed the sample homogenization, while removing moisture and oxidizing the organic matter. All particles showed particles with $dp < 250$ µm and the apparent bulk density ($\rho_{SCBA}$), was greatly decreased from about 2330 kg/m$^3$ (untreated ash, $dp < 500$ µm) to $\rho_{SCBA} = 1400 \pm 10$ kg/m$^3$.

The mineral composition of the sugarcane bagasse ash used in this study is detailed in Table 2. As expected, silica was the major mineral component, reaching almost 60 wt%.
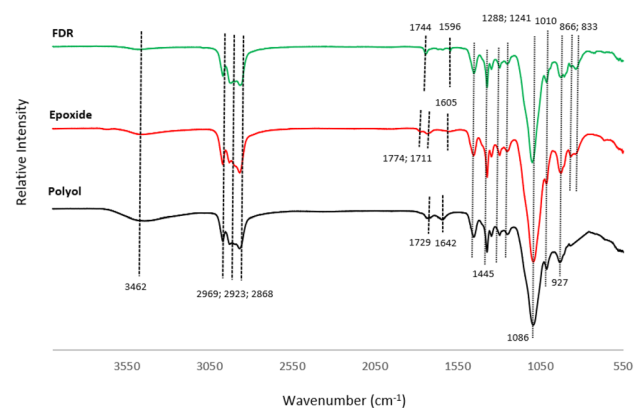


**Fig. 1** Structural analysis (FTIR) reaction progression starting with the oily residue (FDR), the respective epoxide and subsequent polyol

Although the composition is dependent on several factors such as region or local temperature range, sugarcane bagasse is described to have a silica composition ranging from 55 to 90%, and some authors described sugarcane ash with a similar silica concentration [48–51]. Iron oxide was the second most abundant compound in sugarcane ash, corresponding to 17.8 wt %. Although this value is unusually high for this type of biomass, some authors described similar concentrations of iron oxide in sugarcane bagasse, ranging from about 15 to 29 wt% (Patel et al., 2018; Kawade et al., 2013).

## Polyol Characterization

The oily by-product (FDR) from this particular fermentation process, has a highly complex composition [25], containing a polymer (46.5%) derived from the oligomer products of β-farnesene production process, hydrocarbons (43.3% wt), triglycerides (4.2%), diglycerides (2.62%), fatty alcohols (2%), phytosterols (approximately 0.8%), a minimal amount of free fatty acids (0.3%), wax esters (0.2%), and many other compounds.

The reaction yield for the polyol production based on the initial FDR mass, was high ($\eta = 80\%$) which is an important factor attending economic viability.

Polyols reactivity depends upon characteristic properties such as chemical structure, hydroxyl (–OH) value, and acid number and functionality, and the FDR-based polyol (Table 3), presented a molecular weight around 2711.3 Da,

paired with a relatively high functionality (around 4.0), low hydroxyl value (–OH = 82.3 mg KOH/g polyol) and high viscosity at room temperature (13,256 mPa.s).

The hydroxyl value may be highly variable, when comparing with values reported for polyols synthesized from vegetable oils. Examples of that are polyols derived from canola and palm oils with higher –OH values of 267, 222 mg KOH/g of sample, respectively [15], while others polyols obtained from soybean, linseed, and palm oil, exhibited lower values around 90 and 78 mg KOH/g [52, 53]. Those differences may be attributed to different ring-opening agents and reaction conditions used.

With the exception of this FDR-based polyol viscosity, those characteristics, are similar to Basf Lupranol ® 2070 trifunctional polyether polyol with secondary hydroxyl end groups, used for combustion of modified ether slabstock polyurethane foams, with $M_w = 3000$ Da, –OH = 53 mg KOH/g, and viscosity 550 mPa.s [54].

The higher content of oligomers present in the initial feedstock along with the formation of crystallized wax esters at room temperature surely contributed to the high viscosity observed on this polyol [55]. Moreover, phosphoric acid, used in the polyol production, while promoting the ring-opening hydrolysis, connects chemically within the polyol structure creating hydroxyl groups with the ability to form intramolecular H-bonding and higher phosphate esters impacting its viscosity [30, 32, 55].

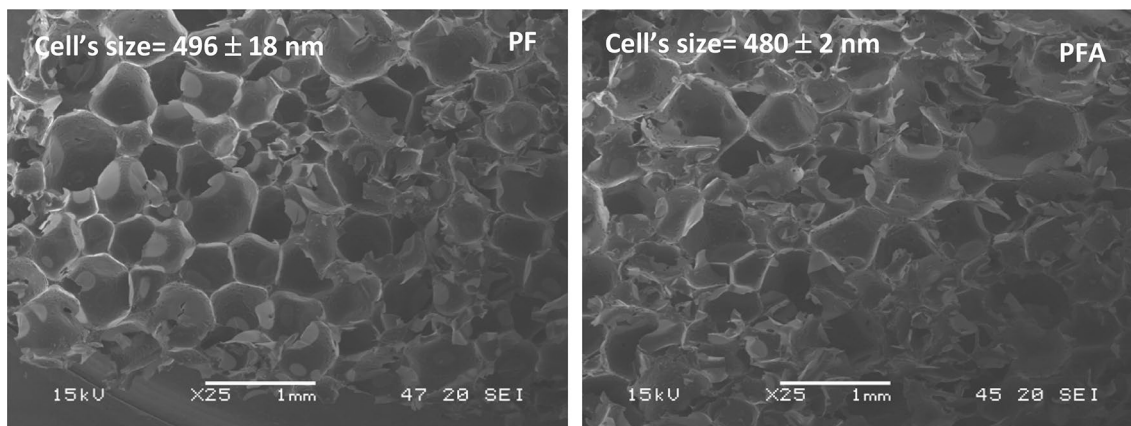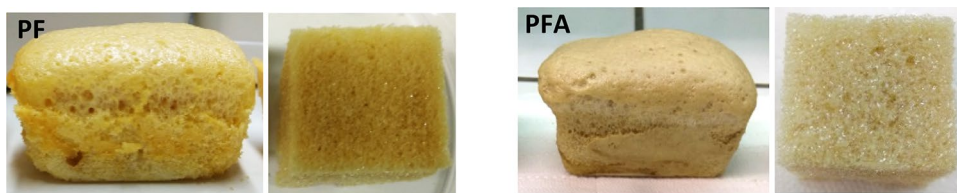**Fig. 2** Representation of both PUR foams (PF and PFA)

**Fig. 3** Representative SEM micrographs of both PUR bio-based foams (PF and PFA), with pore size diameter average values

**Table 4** PUR foams (PF and PFA), density, compressive strength, and specific strength

| Sample | Density (kg/m$^3$) | Compressive strength (kPa) | Specific strength (m$^2$/s$^2$) |
|---|---|---|---|
| PF | 134.7 ± 3.6[a] | 135.9 ± 3.0[a] | 1009 |
| PFA | 105.7 ± 10.1[b] | 121.5 ± 2.3[b] | 1149 |

The ATR-FTIR corroborated by chemical-physical analysis provides significant insight into the molecular structure and chemical composition of all materials. The progression of the polyol synthesis from the feedstock (FDR) is in Fig. 1.

The ATR-FTIR profile of the feedstock FDR (Fig. 1) reveals a mild band between 3200 and 3600 cm$^{-1}$, centered around 3442 cm$^{-1}$, the –OH stretching region. This band is indicative of the presence of hydroxyl groups in the initial feedstock supported by evidence found in previous studies [26] reporting a hydroxyl value (-OH) for FDR of 42.5 mg KOH/g most probably related to the abundance of fatty alcohols and terpenes (such as farnesene and farnesol) in FDR composition [25]. The triple bands in the range 2868–2969 cm$^{-1}$ are assigned to –CH$_2$ and –CH$_3$ symmetrical and asymmetrical stretching and at 1744 cm$^{-1}$ corresponding to the C=O stretching vibrations of ester functional groups present in lipid triglycerides and fatty acids. The strong band at 1088 cm$^{-1}$ indicated the –C–O–C stretching mode [52, 56, 57].

After epoxidation (epoxide profile), a clear evidence of conversion of C=C bonds to epoxy groups/oxirane rings was observed, by the intensification of the two distinctive bands at 866 and 833 cm$^{-1}$ [58]. This fact is corroborated by the reduction of the degree of unsaturation i.e. the iodine value from 130 to 11.3 g I$_2$/100 g recorded in previous work [26]. Additionally, two bands are formed at 1774 cm$^{-1}$ and 1711 cm$^{-1}$, corresponding to the C=O stretching vibrations [52].
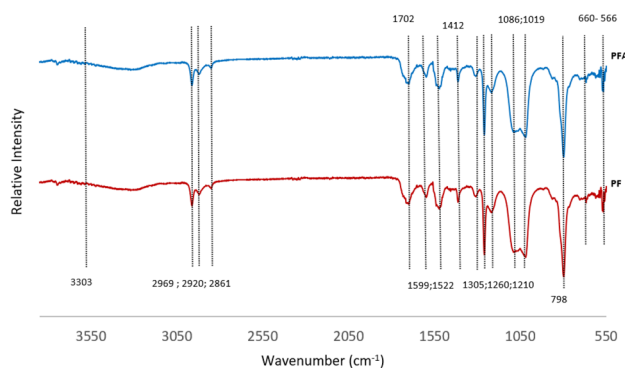
After acid hydrolysis, the polyol profile displays the expected disappearance of the bands 866 and 833 cm$^{-1}$ respective bands oxirane ring-opening and the intensification of the –OH stretching at about 3462 cm$^{-1}$, confirming the attachment of the hydroxyl groups and the final –OH value = 83.2 mg KOH/g [15]. The distinct bands in 1729 and 1642 cm$^{-1}$ are attributed to the –C=O and –C=C– stretching vibrations, respectively [59].

## Foams Characterization

The polyol functionality gives information about chemically active atoms or groups per molecule and the polyol with high values of functionalities (3–5) like this FDR-based polyol ($f$ = 4), are expected to produce rigid foams since they have greater chances of being incorporated into the network due to a great number of reactive sites [60, 61].

The developed bio-based formulations (PF and PFA in Table 1) resulted in rigid polyurethane (PUR) foams easy to cut by a simple saw, releasing small and heavy particles.

A visual inspection (Fig. 2) showed that the reinforced foam (PFA) presented smaller inner cells more homogenously distributed than the neat formulation (PF).

This observation was confirmed by SEM analysis of the foams morphology (Fig. 3) since PF exhibited an average cell's size value of 496 nm and PAF a value of 480 nm.

Observing the representative micrographs, the first visible feature was the irregular structure revealed by both (PF and PFA) conditions, with the latter presenting apparent damage of cells probably caused by ash presence [62, 63]. In addition to the surface heterogeneity, PFA samples displayed micro-holes, in this case, due to the introduction of solid particles into the polyol premix that might significantly alter bubble nucleation conditions, which directly affects the size, shape, and number of pores, as well as pore's wall thickness in the final materials [64]. The finer cell structure, associated to a reduction in foam density after the incorporation of



**Fig. 4** Comparative structural (FTIR) analysis of both PUR foams (PF and PFA)
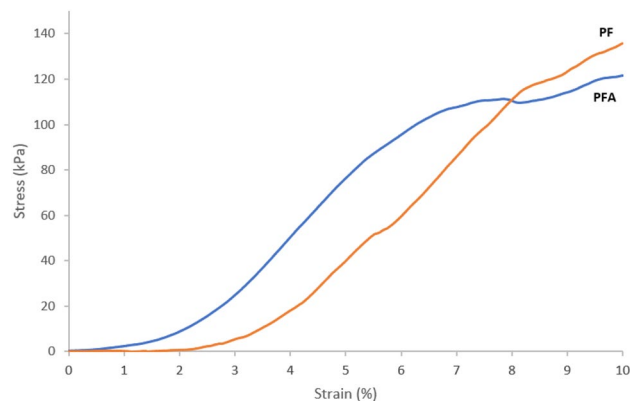


**Fig. 5** Strain–stress curves of both PUR foams (PF and PFA)

particles showed a strong relationship with the increase of nucleating points in the reaction media facilitating, among other things, the process of bubble formation [65–67].

Both bio-based foams exhibited high apparent densities (Table 4) with average values of 134.7 kg/m$^3$ and (PF) and 105.7 kg/m$^3$ (PFA). According to some authors, the filler particles act as nucleation sites that promote an increase in the number of cells formed with increasing filler content therefore promoting a reduction on foam density [20, 68, 69].

The comparative structural analysis between the basic formulation (PF) and the additivated (PFA) (Fig. 4), showed that the polyol related –OH stretching band at 3462 cm$^{-1}$ (Fig. 1) disappeared and new bands emerged following the reaction between –OH, –NCO (from 4,4- MDI) and additives. For instance, at 3309 cm$^{-1}$ it was detected a band assigned to -NH stretching, as well C=O stretching (amide I) band at 1702 cm$^{-1}$, the amide II band at 1507–1540 cm$^{-1}$ and the amide III band at 1210–1260 cm$^{-1}$. Bands characteristic of C–O stretching of the carbonate group emerged at 1210 and 1260 cm$^{-1}$ along with 798 cm$^{-1}$ characteristic out-of-plane bending of O–CO–O and 1599 cm$^{-1}$ (C–C stretching) of benzene ring. The three bands presented in the range 2969 and 2860 (asymmetric and symmetric C–H stretching) remain [70, 71]. This analysis corroborates the expected results according to previously published articles for this type of material [69, 72, 73].

The spectrum of the ash-filled foam (PFA) overlapped with the spectrum of the plain foam (PF) (Fig. 4).

Both formulations exhibited similar bands and intensities without additional bands that belong to other chemical species, suggesting that sugarcane bagasse ash was not chemically bound to the polymer and consequently not incor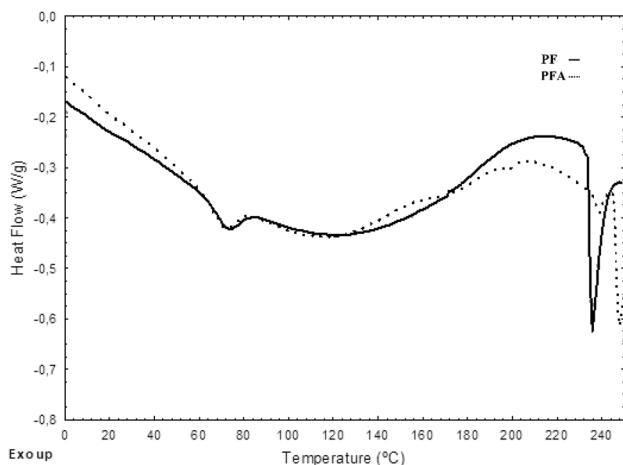porated in the molecular structure. Several results were reported for polyurethane made with fly ash, where only slight changes were observed in the composite foam spectrum with additional bands at about 680, 610, 595 and 460 cm$^{-1}$ from the presence of aluminosilicate and silica [19].

Looking into the comparative stress–strain plot (Fig. 5), both foams showed the usual linear elastic region, yet PF behavior surpassed the typical plateau phase, progressing immediately to a steep increase in stress indicative of the densification of the collapsed cell's walls [74]. PFA displayed a milder progression suggesting a plateau phase at higher strain rates [75].

The compressive strength values (Table 4) at 10% strain were 135.9 kPa (PF) and 121.5 kPa (PFA).

These results are weak within this density range when comparing with foams made with sustainable Mannich polyols and natural fillers such as powdered walnut shell with foam density 111.53 ± 8.66 kg/m3 and compressive strength of 0.38 ± 0.02 MPa [72] or fossil-based foams with 5% of fly ash (diameter below 25 mm) with apparent density of 40.5 ± 0.6 kg/m$^3$ corresponding to a compressive strength of 205.89 ± 16.86 kPa [19].

Incorporating only 4.5% SCBA (grain size below 250 μm) was ineffective in the increment of the compressive strength, however, that small amount was enough to increase the foam's specific strength from 1009 to 1149 m$^2$/s$^2$, suggesting that other factors (e.g. polyol composition, grain size, ash packing, etc.) are yet to be accounted.

It was observed in previous experiments, that the addition of higher percentages of ash resulted in an exponential increase in the polyol premix viscosity, inducing filler agglomeration, hindering foam rising, resulting in foams with very fragile structures, effects also observed in similar studies [20, 62]. The incorporation of 4.5% of ashes in the polyurethane foam was considered a hard limit and the synthesis was optimized accordingly.

Furthermore, ester-based polyols are usually more viscous and FDR-based polyol is an example (about 13,256 mPa.s at room temperature) a factor that strongly affected polyurethane processability in laboratory conditions [76]. Recalling the FDR lipidic composition [25] and the derived polyol characterization (Table 3), that high viscosity is most probably due to the presence of epoxide oligomers that form hydrogen bonds in the presence of the hydroxyl groups generated in the ring-opening reaction [77] and the



**Fig. 6** Comparative thermogram (DSC) of both PUR foams (PF and PFA)

**Table 5** PUR foams (PF and PFA), thermal properties (T$_g$, T$_d$ and k)

| Sample | T$_g$ (°C) | T$_d$ (°C) | k (W/m.K) |
| --- | --- | --- | --- |
| PF | 74.0 | 215.0–238.0 | 0.0482 ± 0.0002 |
| PFA | 71.8 | 230.0–247.0 | 0.0461 ± 0.0001 |

**Table 6** PUR foams (PF and PFA) flammability evaluation. Horizontal burning test results

| Samples | Burning time after flame | Burning length | Time extinguishment | PMR | Burning rate |
|---|---|---|---|---|---|
| | (s) | (mm) | (s) | (%) | (mm/min) |
| PF | $251.7 \pm 41.7$ | $132.3 \pm 2.1$ | $255.0 \pm 49.5$ | $57.4 \pm 6.3$ | $33 \pm 6$ |
| PFA | $90.3 \pm 24.5$ | $56.7 \pm 17.0$ | $116.7 \pm 17.0$ | $87.4 \pm 7.8$ | $38 \pm 6$ |

T extinguishment- time between application of burner flame and specimen flame extinguishment, s. Afterglow shall not be included in this time. PMR- percentual mass retained by the entire specimen. PMR = (S2/S1) × 100, where S2 is the mass of specimen after ignition (g) and S1 before ignition (g)



**Fig. 7** Pictures of both PUR foams, PF and PFA, after flammability tests

presence of waxes with crystallization temperature above room temperature [76].

On top of that, cross-linking vegetable-oil derived polyols with MDI can be compromised by steric hindrance introduced by the presence of secondary hydroxyl groups and long dangling hydrocarbon chains, affecting negatively the polymer network resistance to stress under load [78–80]. To improve the incorporation of this viscous polyol in the foam premix it was necessary to use heat, and the carbon dioxide ($CO_2$) gas bubbles released by reaction with the diisocyanate were trapped when the highly viscous mixture had cooled, restraining the expansion of cell's hence conditioning its size and distribution, and therefore foam density and compressive strength [20, 77, 81, 82].

The incorporation of natural oils in polyol synthesis is generally associated with some difficulties in the formulation of polyurethane foams due to their functionality, high viscosity, and low hydroxyl numbers that may affect foam properties like stability, strength, and glass transition [83, 84]. However, these materials have a versatile composition, are biodegradable, nontoxic, and environmentally friendly [85].

Observing the comparative thermogram obtained by DSC (Fig. 6), both PF and PFA exhibited overlapped intervals of decomposition onset temperatures related to the bio-polyol backbone in both materials, suggesting that sugarcane bagasse ash wasn't integrated in the polyurethane molecular structure [86].

In Table 5, the different thermal events are identified, namely the glass transition temperature ($T_g$) and the

decomposition onset temperatures ($T_d$), which is indicative of initial thermal degradation. $T_g$ values of 74.0 and 71.8 °C were found for both PF and PFA polyurethanes respectively, with a slight decrease associated with the incorporation of ash content. Those $T_g$ values are close to the values previously reported by similar studies [87, 88]. The decomposition onset temperatures were observed as narrow endothermic peaks in both samples above 200 °C, indicating the beginning of thermal degradation, at 215.0 and 230.0 °C for PA and PFA conditions, respectively. For the reinforced foam, an endothermic peak was observed at a higher temperature (247.0 °C) which may be related to the presence of silica (2.7% wt) in the ash.

Thermal conductivity is mainly the result of a balance between the blowing gas content (e.g. $CO_2$ or other), foam density and cell's size [89, 90], and inert fillers that act as nucleating agents are often used to control cell's size [91]. This fact was confirmed even with this limited amount of ash by the thermal conductivity values (Table 5), 0.0482 W/.m.K (PF), and 0.0461 W/m.K (PFA). Similar results were described in a study conducted with tung oil-based polyol and rice husk ash up to 5% [20]. These values are within the range of inorganic compounds like ceramics, cellular calcium silicate or glass as well natural fibers such as rice straw, wood and coconut fibers or cork without the inherent sensitivity to moisture [92].

The analysis of all compiled data (foams structure, mechanical and thermal properties) suggest that ash particles are only physically attached to the polymer structure promoting a higher polymer chain mobility, thus reducing the thermal conductivity, decreasing the glass transition temperature, delaying the decomposition onset temperature, while slightly reducing the compressive strength [93].

The thermal conductivity for both bio-based foams was in the range of inorganic compounds such as ceramics, cellular calcium silicate, or cellular glass, along with natural fibers (e.g. coconut and cork), without the inherent sensitivity to moisture [94].

The flammability test results, compiled in Table 6, will be one of the limiting factors for a potential application as thermal insulation material. The specimens after the ignitability test under open flame are represented in Fig. 7.

The neat foam (PF) exhibited a higher burning length (132.3 mm), burning time (251.7 s), and time of extinguishment (255.0 s) than the filled foam (56.7 mm, 90.3 s and

116.7 s, respectively). The remaining amount of sample after burning was about 57.4% for PF and 87.4% for PFA, respectively, despite the higher burning rate of PFA (38 mm min$^{-1}$) compared with PF (33 mm min$^{-1}$). Materials with rating HB by UL 94 standard for safety shall not have a burning rate exceeding 40 mm per minute over a 75 mm span for specimens having a thickness of 3.0 to 13 mm or cease to burn before the 100 mm reference mark. Both criteria were accomplished by the ash-filled foam.

It has been reported that ash from wastes rich in Si and Ca elements which are assigned for $SiO_2$ and $CaCO_3$, respectively, had a positive effect on flame retardancy of PU foams [22, 95, 96]. These results were in accordance with this work, since silica ($SiO_2$) was the predominant mineral in the added ash accounting for 59.5% wt (Table 2) and the addition of 4.5% SCBA to the foam formulation, amount to a total of 2.7% wt in $SiO_2$. The compound $Fe_2O_3$ was the second most abundant (17% wt) in SCBA, and it was also tested for its flame-retardant potential in previous works. Hollow glass microspheres coated with $Fe_2O_3$ enhanced the flame retardant and smoke suppression in thermoplastic polyurethane [97]. In another work, when $Fe_2O_3$ particles were used in a mixture with PET at 1.2%, the limiting oxygen index increased by around 6%, the total heat release and smoke production decreased by 32% and 57%, respectively [98].

## Conclusions

Rigid polyurethane water-blown foams were successfully produced based on the valorization of two by-products derived from Amyris industrial fermentation process, the microbial crude oil recovered after distillation, and sugarcane bagasse ash obtained from the cogeneration unit.

Polyurethane formulation was particularly challenging since the backbone is a polyol derived from a biowaste with a biphasic composition, prone to epoxide oligomerization and wax crystallization.

FTIR analysis showed the typical bands expected for polyurethane foams, while microscopic observations showed a well-formed finer structure, albeit heterogeneous, paired with a lower foam density of the filled foam, suggesting that ash particles acted as nucleation sites during the foaming process promoting structural stabilization while reducing foam's density, cell's size, and thermal conductivity.

Within the high density range, both foams showed a relatively low mechanical performance suggesting that controlling polyol viscosity, hence foam porosity, particle size, and distribution in the matrix are crucial points. An adequate pretreatment of the microbial oil and implementing changes in the reaction system should impart improved results.

The absence of chemical interaction between ash filler and the polyurethane matrix and foam structure suggests that ash as a filler has a plasticizing effect increasing the polymer chain mobility, thus decreasing the glass transition temperature of the foam, delaying the decomposition onset temperature.

The flammability test results suggest that sugarcane bagasse ash has improved the foam performance (burning time, time of extinguishment, and burning length), in compliance with the fire protection standard UL 94, class HB.

Notwithstanding the need for further improvement and more in-depth evaluation of flammability properties the results corroborate the idea that polyurethane foams derived from suitable and renewable waste by-products constitute a sustainable green alternative to both edible and fossil-based sources and that sugarcane bagasse ash can be an acceptable source of silica for the reinforcement of composites with reduced flammability eventually replacing harmful halogenated chemicals used with the same purpose.

**Data Availability** Enquiries about data availability should be directed to the authors.

## Declarations

**Conflict of interest** The authors declare no conflict of interest.

**Statement of Novelty** In this groundbreaking study, we unveil an innovative approach to enhance the fire-retardancy and thermal characteristics of rigid bio-based polyurethane foam using two unique industrial byproducts. These by-products, namely microbial oil derived from the industrial production of β-farnesene and sugarcane bagasse ash, play a pivotal role in augmenting the performance of the foam. As the world witnesses a surging global interest in transitioning from conventional fossil-based polymers to sustainable materials derived from organic or inorganic waste sources, along with the incorporation of filler-type additives that align with environmental sustainability goals, our research findings hold profound significance.

# References

1. Morseletto, P.: Targets for a circular economy. Resour. Conserv. Recycl. **153**, 104553 (2020). https://doi.org/10.1016/j.resconrec.2019.104553

2. Höök, M., Davidsson, S., Johansson, S., Tang, X.: Decline and depletion rates of oil production: a comprehensive investigation. Philos. Trans. R Soc. A Math. Phys. Eng. Sci. **372**, 20120448 (2014). https://doi.org/10.1098/rsta.2012.0448

3. Sorrell, S., Speirs, J., Bentley, R., Brandt, A., Miller, R.: Global oil depletion: a review of the evidence. Energy Policy **38**, 5290–5295 (2010). https://doi.org/10.1016/j.enpol.2010.04.046

4. Di Bartolo, A., Infurna, G., Dintcheva, N.T.: A review of bioplastics and their adoption in the circular economy. Polymers (Basel) (2021). https://doi.org/10.3390/polym13081229

5. Waghmare, B., Mahanwar, P., Waghmare, B., Mahanwar, P.: Review on synthesis of isocyanate free polyurethane using sustainable routes and its applications Reprinted from PAINTINDIA May 2019 Review on synthesis of isocyanate free polyurethane using sustainable routes and its applications. (2019)

6. Das, A., Mahanwar, P.: A brief discussion on advances in polyurethane applications. Adv. Ind. Eng. Polym. Res. **3**, 93–101 (2020). https://doi.org/10.1016/j.aiepr.2020.07.002

7. Shoaib, S., Shahzad Maqsood, K., Nafisa, G., Waqas, A., Muhammad, S., Tahir, J.: A comprehensive short review on polyurethane foam. Int. J. Innov. Appl. Stud. **12**, 165–169 (2014)

8. Berardi, U.: The impact of aging and environmental conditions on the effective thermal conductivity of several foam materials. Energy **182**, 777–794 (2019). https://doi.org/10.1016/j.energy.2019.06.022

9. Wittbecker, W., Daems; D., Werther, U.: Performance of polyurethane (PUR) building products in fires, https://www.isopa.org/media/1136, (2011)

10. Tenorio-Alfonso, A., Sánchez, M.C., Franco, J.M.: A Review of the sustainable approaches in the production of bio-based polyurethanes and their applications in the adhesive field. J. Polym. Environ. **28**, 749–774 (2020). https://doi.org/10.1007/s10924-020-01659-1

11. Kaikade, D.S., Sabnis, A.S.: Polyurethane foams from vegetable oil-based polyols: a review. Polym. Bull. **80**, 2239–2261 (2023). https://doi.org/10.1007/s00289-022-04155-9

12. Patil, C.K., Jung, D.W., Jirimali, H.D., Baik, J.H., Gite, V.V., Hong, S.C.: Nonedible vegetable oil-based polyols in anticorrosive and antimicrobial polyurethane coatings. Polymers (Basel) **13**, 3149 (2021). https://doi.org/10.3390/polym13183149

13. Dang, Y., Luo, X., Wang, F., Li, Y.: Value-added conversion of waste cooking oil and post-consumer PET bottles into biodiesel and polyurethane foams. Waste Manag. **52**, 360–366 (2016). https://doi.org/10.1016/j.wasman.2016.03.054

14. Athawale, V.D., Nimbalkar, R.V.: Polyurethane dispersions based on sardine fish oil, soybean oil, and their interesterification products. J. Dispers. Sci. Technol. **32**, 1014–1022 (2011). https://doi.org/10.1080/01932691.2010.497459

15. Uprety, B.K., Reddy, J.V., Dalli, S.S., Rakshit, S.K.: Utilization of microbial oil obtained from crude glycerol for the production of polyol and its subsequent conversion to polyurethane foams. Bioresour. Technol. **235**, 309–315 (2017). https://doi.org/10.1016/j.biortech.2017.03.126

16. Samavi, M., Rakshit, S.: Utilization of microbial oil from poplar wood hemicellulose prehydrolysate for the production of polyol using chemo-enzymatic epoxidation. Biotechnol. Bioprocess Eng. **25**, 327–335 (2020). https://doi.org/10.1007/s12257-019-0416-8

17. Ramanujam, S., Zequine, C., Bhoyate, S., Neria, B., Kahol, P., Gupta, R.: Novel biobased polyol using corn oil for highly flame-retardant polyurethane foams. C **5**, 13 (2019). https://doi.org/10.3390/c5010013

18. Mngomezulu, M.E., John, M.J., Jacobs, V., Luyt, A.S.: Review on flammability of biofibres and biocomposites. Carbohydr. Polym. **111**, 149–182 (2014). https://doi.org/10.1016/j.carbpol.2014.03.071

19. Kuźnia, M., Magiera, A., Pielichowska, K., Ziąbka, M., Benko, A., Szatkowski, P., Jerzak, W.: Fluidized bed combustion fly ash as filler in composite polyurethane materials. Waste Manag. **92**, 115–123 (2019). https://doi.org/10.1016/j.wasman.2019.05.012

20. Ribeiro Da Silva, V., Mosiewicki, M.A., Yoshida, M.I., Coelho Da Silva, M., Stefani, P.M., Marcovich, N.E.: Polyurethane foams based on modified tung oil and reinforced with rice husk ash I: synthesis and physical chemical characterization. Polym. Test. **32**, 438–445 (2013). https://doi.org/10.1016/j.polymertesting.2013.01.002

21. Ali, M.H.M., Rahman, H.A., Amirnordin, S.H., Khan, N.A.: Eco-friendly flame-retardant additives for polyurethane foams: a short review. Key Eng. Mater. **791**, 19–28 (2018). https://doi.org/10.4028/www.scientific.net/KEM.791.19

22. Kairytė, A., Kremensas, A., Vaitkus, S., Członka, S., Strąkowska, A.: Fire suppression and thermal behavior of biobased rigid polyurethane foam filled with biomass incineration waste ash. Polymers (Basel) **12**, 683 (2020). https://doi.org/10.3390/polym12030683

23. Licht, S.: Chapter 5—Fermentation for Biofuels and Bio-Based Chemicals. In: Vogel, H.C. (ed.) Fermentation and Biochemical Engineering Handbook, pp. 59–82. Elsevier, Amsterdam (2014)

24. Benjamin, K.R., Silva, I.R., Cherubim, J.P., McPhee, D., Paddon, C.J.: Developing commercial production of semi-synthetic artemisinin, and of β-Farnesene, an isoprenoid produced by fermentation of Brazilian sugar. J. Braz. Chem. Soc. **27**, 1339–1345 (2016). https://doi.org/10.5935/0103-5053.20160119

25. Teixeira, F.S., Vidigal, S.S.M.P., Pimentel, L.L., Costa, P.T., Tavares-Valente, D., Azevedo-Silva, J., Pintado, M.E., Fernandes, J.C., Rodríguez-Alcalá, L.M.: Phytosterols and novel triterpenes recovered from industrial fermentation coproducts exert In vitro anti-inflammatory activity in macrophages. Pharmaceuticals **14**, 583 (2021). https://doi.org/10.3390/ph14060583

26. Capêto, A.P., Azevedo-Silva, J., Sousa, S., Pintado, M., Guimarães, A.S., Oliveira, A.L.S.: Synthesis of Bio-based polyester from microbial lipidic residue intended for biomedical application. Int. J. Mol. Sci. **24**, 4419 (2023). https://doi.org/10.3390/ijms24054419

27. Li, Y.Y., Luo, X., Hu, S.: Bio-based Polyols and Polyurethanes. Springer, Cham (2015). https://doi.org/10.1007/978-3-319-21539-6

28. Hattimattur, V., Sangale, V.R., Zade, P.S., Mandake, M.B., Walke, S., Mumbai, N.: Review: epoxidation of vegetable oils. Int. J. Trend Res. Dev. **5**, 542–548 (2018)

29. Abril-Milán, D., Valdés, O., Mirabal-Gallardo, Y., de la Torre, A.F., Bustamante, C., Contreras, J.: Preparation of renewable bio-polyols from two species of colliguaja for rigid polyurethane foams. Materials (Basel). **11**, 1–20 (2018). https://doi.org/10.3390/ma11112244

30. Guo, Y., Hardesty, J.H., Mannari, V.M., Massingill, J.L.: Hydrolysis of epoxidized soybean oil in the presence of phosphoric acid. JAOCS. J. Am. Oil Chem. Soc. **84**, 929–935 (2007). https://doi.org/10.1007/s11746-007-1126-5

31. Pfister, D.P., Xia, Y., Larock, R.C.: Recent advances in vegetable oil-based polyurethanes. Chemsuschem **4**, 703–717 (2011). https://doi.org/10.1002/cssc.201000378

32. Meshram, P.D., Patil, H.V., Puri, R.G.: Producing phosphate-polyols by ring-opening hydrolysis of wild safflower oil epoxides. Int. J. ChemTech Res. **10**, 206–215 (2017)

33. Niyogi, D., Kumar, R., Gandhi, K.S.: Water blown free rise polyurethane foams. Polym. Eng. Sci. **39**, 199–209 (1999). https://doi.org/10.1002/pen.11408

34. Ionescu, M.: Chemistry and Technology of Polyols for Polyurethane, vol. 2. Rapra Publishing (2016). https://doi.org/10.1002/pi.2159

35. ASTM International: ASTM D7481-18 Standard Test Methods for Determining Loose and Tapped Bulk Densities of Powders using a Graduated Cylinder (2018). https://doi.org/10.1520/D7481-18

36. ASTM International: ASTM C136/C136M-19, Standard Test Method for Sieve Analysis of Fine and Coarse Aggregates (2019). https://doi.org/10.1520/C0136_C0136M-19

37. ASTM International: ASTM D4662-20, Standard Test Methods for Testing Polyurethane Raw Materials: Determination of Acid and Alkalinity Numbers of Polyols. West Conshohocken, PA, USA (2020). https://doi.org/10.1520/D4662-20

38. ASTM International: ASTM E222-17, Standard Test Methods for Hydroxyl Groups Using Acetic Anhydride Acetylation (2017). https://doi.org/10.1520/E0222-17

39. ASTM International: ASTM D 4678-15, Standard Test Methods for Polyurethane Raw Materials: Determination of Viscosity of Polyols, Annual Book of ASTM Standards (2015). https://doi.org/10.1520/D4878-15.2

40. Bahurudeen, A., Kanraj, D., Gokul Dev, V., Santhanam, M.: Performance evaluation of sugarcane bagasse ash blended cement in concrete. Cem. Concr. Compos. **59**, 77–88 (2015). https://doi.org/10.1016/j.cemconcomp.2015.03.004

41. Xu, Q., Ji, T., Gao, S.-J., Yang, Z., Wu, N.: Characteristics and applications of sugar cane bagasse ash waste in cementitious materials. Materials (Basel) **12**, 39 (2018). https://doi.org/10.3390/ma12010039

42. Patel, H.: Environmental valorisation of bagasse fly ash: a review. RSC Adv. **10**, 31611–31621 (2020). https://doi.org/10.1039/D0RA06422J

43. Micheal, A., Moussa, R.R.: Investigating the economic and environmental effect of integrating sugarcane bagasse (SCB) fibers in cement bricks. Ain Shams Eng. J. **12**, 3297–3303 (2021). https://doi.org/10.1016/j.asej.2020.12.012

44. Barrera Torres, G., Dognani, G., da Silva Agostini, D.L., dos Santos, R.J., Camargo Cabrera, F., Gutierrez Aguilar, C.M., de Paiva, F.F.G., Rainho Teixeira, S., Job, A.E.: Potential eco-friendly application of sugarcane bagasse ash in the rubber industry. Waste Biomass Valoriz. **12**, 4599–4613 (2021). https://doi.org/10.1007/s12649-020-01309-6

45. Usta, N.: Investigation of fire behavior of rigid polyurethane foams containing fly ash and intumescent flame retardant by using a cone calorimeter. J. Appl. Polym. Sci. **124**, 3372–3382 (2012). https://doi.org/10.1002/app.35352

46. Costa, J.R., Capeto, A.P., Pereira, C.F., Pedrosa, S.S., Mota, I.F., Burgal, J.S., Pintado, A.I., Pintado, M.E., Oliveira, C.S.S., Costa, P., Madureira, A.R.: Valorization of sugarcane by-products through synthesis of biogenic amorphous silica microspheres for sustainable cosmetics. Nanomaterials (2022). https://doi.org/10.3390/nano12234201

47. Jesus, M., Teixeira, J., Alves, J.L., Pessoa, S., Guimarães, A.S., Rangel, B.: Potential Use of Sugarcane Bagasse Ash in Cementitious Mortars for 3D Printing. In: da Silva, L.F.M. (ed.) Advanced Structured Materials book series, vol. 168, pp. 89–103. Springer, Switzerland (2023)

48. Rovani, S., Santos, J.J., Corio, P., Fungaro, D.A.: Highly pure silica nanoparticles with high adsorption capacity obtained from sugarcane waste ash. ACS Omega **3**, 2618–2627 (2018). https://doi.org/10.1021/acsomega.8b00092

49. Souza, A.E., Teixeira, S.R., Santos, G.T.A., Costa, F.B., Longo, E.: Reuse of sugarcane bagasse ash (SCBA) to produce ceramic materials. J. Environ. Manag. **92**, 2774–2780 (2011). https://doi.org/10.1016/j.jenvman.2011.06.020

50. Jiménez-Quero, V.G., León-Martínez, F.M., Montes-García, P., Gaona-Tiburcio, C., Chacón-Nava, J.G.: Influence of sugar-cane bagasse ash and fly ash on the rheological behavior of cement pastes and mortars. Constr. Build. Mater. **40**, 691–701 (2013). https://doi.org/10.1016/j.conbuildmat.2012.11.023

51. Khalil, M.G., Aslam, M., Ahmad, S.: Utilization of sugarcane bagasse ash as cement replacement for the production of sustainable concrete – A review. Construct. Build. Mater. 270, 121371 (2021). https://doi.org/10.1016/j.conbuildmat.2020.121371

52. Cifarelli, A., Boggioni, L., Vignali, A., Tritto, I., Bertini, F., Losio, S.: Flexible polyurethane foams from epoxidized vegetable oils and a bio-based diisocyanate. Polymers (Basel) **13**, 612 (2021). https://doi.org/10.3390/polym13040612

53. Ang, K.P., Lee, C.S., Cheng, S.F., Chuah, C.H.: Synthesis of palm oil-based polyester polyol for polyurethane adhesive production. J. Appl. Polym. Sci. (2014). https://doi.org/10.1002/app.39967

54. Basf Corporation: Lupranol ® 2070 Technical Data Sheet (2017). https://chemicals.basf.com/global/monomers/tds_isocyanate/lupranol/Lupranol%202070.pdf

55. Coman, A.E., Peyrton, J., Hubca, G., Sarbu, A., Gabor, A.R., Nicolae, C.A., Iordache, T.V., Averous, L.: Synthesis and characterization of renewable polyurethane foams using different biobased polyols from olive oil. Eur. Polym. J. **149**, 110363 (2021). https://doi.org/10.1016/j.eurpolymj.2021.110363

56. Mihoubi, W., Sahli, E., Gargouri, A., Amiel, C.: FTIR spectroscopy of whole cells for the monitoring of yeast apoptosis mediated by p53 over-expression and its suppression by Nigella sativa extracts. PLoS ONE (2017). https://doi.org/10.1371/journal.pone.0180680

57. Shapaval, V., Afseth, N.K., Vogt, G., Kohler, A.: Fourier transform infrared spectroscopy for the prediction of fatty acid profiles in Mucor fungi grown in media with different carbon sources. Microb. Cell Fact. **13**, 1–11 (2014). https://doi.org/10.1186/1475-2859-13-86

58. Jalil, M.J., Md Zaini, M.S., Mohd Yamin, A.F., Azmi, I.S., Chang, S.H., Morad, N., Hadi, A.: Synthesis and physicochemical properties of epoxidized oleic acid-based palm oil. IOP Conf. Ser. Earth Environ. Sci. **291**, 012046 (2019). https://doi.org/10.1088/1755-1315/291/1/012046

59. Coates, J.: Encyclopedia of analytical chemistry-Interpretation of infrared spectra, a practical approach. Encycl. Anal. Chem. 1–23 (2004)

60. Zieleniewska, M., Leszczyński, M.K., Kurańska, M., Prociak, A., Szczepkowski, L., Krzyżowska, M., Ryszkowska, J.: Preparation and characterisation of rigid polyurethane foams using a rapeseed oil-based polyol. Ind. Crops Prod. **74**, 887–897 (2015). https://doi.org/10.1016/j.indcrop.2015.05.081

61. Lu, Y., Larock, R.C.: Soybean-oil-based waterborne polyurethane dispersions: effects of polyol functionality and hard segment content on properties. Biomacromol **9**, 3332–3340 (2008). https://doi.org/10.1021/bm801030g

62. Uram, K., Kurańska, M., Andrzejewski, J., Prociak, A.: Rigid polyurethane foams modified with biochar. Materials (Basel). **14**, 1–14 (2021). https://doi.org/10.3390/ma14195616

63. Kuźnia, M., Zygmunt-Kowalska, B., Szajding, A., Magiera, A., Stanik, R., Gude, M.: Comparative study on selected properties of modified polyurethane foam with fly ash. Int. J. Mol. Sci. (2022). https://doi.org/10.3390/ijms23179725

64. Leszczyńska, M., Malewska, E., Ryszkowska, J., Kurańska, M., Gloc, M., Leszczyński, M.K., Prociak, A.: Vegetable fillers and rapeseed oil-based polyol as natural raw materials for the production of rigid polyurethane foams. Materials (Basel) 14, 1772 (2021). https://doi.org/10.3390/ma14071772

65. Merillas, B., Villafañe, F., Rodríguez-Pérez, M.Á.: Nanoparticles addition in PU foams: the dramatic effect of trapped-air on nucleation. Polymers (Basel). 13, 2952 (2021). https://doi.org/10.3390/polym13172952

66. Lorusso, C., Vergaro, V., Monteduro, A., Saracino, A., Ciccarella, G., Congedo, P.M., Scremin, B.F.: Characterization of polyurethane foam added with synthesized acetic and oleic-modified Tio2 nanocrystals. Nanomater. Nanotechnol. 5, 26 (2015). https://doi.org/10.5772/61275

67. Chen, Y., Das, R., Battley, M.: Effects of cell size and cell wall thickness variations on the strength of closed-cell foams. Int. J. Eng. Sci. 120, 220–240 (2017). https://doi.org/10.1016/j.ijengsci.2017.08.006

68. Akkoyun, M., Akkoyun, S.: Blast furnace slag or fly ash filled rigid polyurethane composite foams: a comprehensive investigation. J. Appl. Polym. Sci. (2019). https://doi.org/10.1002/app.47433

69. Hejna, A., Kopczyńska, M., Kozłowska, U., Klein, M., Kosmela, P., Piszczyk, Ł: Foamed polyurethane composites with different types of ash – morphological, mechanical and thermal behavior assessments. Cell. Polym. 35, 287–308 (2016). https://doi.org/10.1177/026248931603500601

70. Jiang, L., Ren, Z., Zhao, W., Liu, W., Liu, H., Zhu, C.: Synthesis and structure/properties characterizations of four polyurethane model hard segments. R. Soc. Open Sci. (2018). https://doi.org/10.1098/rsos.180536

71. Rogulska, M., Kultys, A., Pikus, S.: The effect of chain extender structure on the properties of new thermoplastic poly(carbonate–urethane)s derived from MDI. J. Therm. Anal. Calorim. 127, 2325–2339 (2017). https://doi.org/10.1007/s10973-016-5756-4

72. De Luca Bossa, F., Santillo, C., Verdolotti, L., Campaner, P., Minigher, A., Boggioni, L., Losio, S., Coccia, F., Iannace, S., Lama, G.C.: Greener nanocomposite polyurethane foam based on sustainable polyol and natural fillers: investigation of chemicophysical and mechanical properties. Materials (Basel) 13, 211 (2020). https://doi.org/10.3390/ma13010211

73. Kuźnia, M., Magiera, A., Zygmunt-Kowalska, B., Kaczorek-Chrobak, K., Pielichowska, K., Szatkowski, P., Benko, A., Ziabka, M., Jerzak, W.: Fly ash as an eco-friendly filler for rigid polyurethane foams modification. Materials (Basel) 14 (2021). https://doi.org/10.3390/ma14216604

74. Mane, J.V., Chandra, S., Sharma, S., Ali, H., Chavan, V.M., Manjunath, B.S., Patel, R.J.: Mechanical property evaluation of polyurethane foam under quasi-static and dynamic strain rates-an experimental study. Procedia Eng. 173, 726–731 (2017). https://doi.org/10.1016/j.proeng.2016.12.160

75. Tu, Z.H., Shim, V.P.W., Lim, C.T.: Plastic deformation modes in rigid polyurethane foam under static loading. Int. J. Solids Struct. 38, 9267–9279 (2001). https://doi.org/10.1016/S0020-7683(01)00213-X

76. Marcovich, N.E., Kurańska, M., Prociak, A., Malewska, E., Bujok, S.: The effect of different palm oil-based bio-polyols on foaming process and selected properties of porous polyurethanes. Polym. Int. 66, 1522–1529 (2017). https://doi.org/10.1002/pi.5408

77. Ji, D., Fang, Z., He, W., Luo, Z., Jiang, X., Wang, T., Guo, K.: Polyurethane rigid foams formed from different soy-based polyols by the ring opening of epoxidised soybean oil with methanol, phenol, and cyclohexanol. Ind. Crops Prod. 74, 76–82 (2015). https://doi.org/10.1016/j.indcrop.2015.04.041

78. Narine, S.S., Kong, X., Bouzidi, L., Sporns, P.: Physical properties of polyurethanes produced from polyols from seed oils: II. Foams. JAOCS. J. Am. Oil Chem. Soc. 84, 65–72 (2007). https://doi.org/10.1007/s11746-006-1008-2

79. Pillai, P.K.S., Li, S., Bouzidi, L., Narine, S.S.: Metathesized palm oil polyol for the preparation of improved bio-based rigid and flexible polyurethane foams. Ind. Crops Prod. 83, 568–576 (2016). https://doi.org/10.1016/j.indcrop.2015.12.068

80. Prociak, A., Kurańska, M., Uram, K., Wójtowicz, M.: Bio-polyurethane foams modified with a mixture of bio-polyols of different chemical structures. Polymers (Basel) 13, 2469 (2021). https://doi.org/10.3390/polym13152469

81. Sundang, M., Nurdin, N.S., Saalah, S., Singam, Y.J., Al Edrus, S.S.A.O., Ismail, N.M., Sipaut, C.S., Abdullah, L.C.: Synthesis of jatropha-oil-based polyester polyol as sustainable biobased material for waterborne polyurethane dispersion. Polymers (Basel) (2022). https://doi.org/10.3390/polym14183715

82. Dzulkifli, M.H., Yahya, M.Y., Md Akhir, F.S., Majid, R.A.: Development of rigid biocomposite polyurethane foam for load bearing application. J. Teknol 68, 53–56 (2014). https://doi.org/10.11113/jt.v68.2929

83. Ghasemlou, M., Daver, F., Ivanova, E.P., Adhikari, B.: Polyurethanes from seed oil-based polyols: a review of synthesis, mechanical and thermal properties. Ind. Crops Prod. 142, 111841 (2019). https://doi.org/10.1016/j.indcrop.2019.111841

84. Echeverria-Altuna, O., Ollo, O., Larraza, I., Gabilondo, N., Harismendy, I., Eceiza, A.: Effect of the biobased polyols chemical structure on high performance thermoset polyurethane properties. Polymer (Guildf) 263, 125515 (2022). https://doi.org/10.1016/j.polymer.2022.125515

85. Dhaliwal, G.S., Anandan, S., Chandrashekhara, K., Lees, J., Nam, P.: Development and characterization of polyurethane foams with substitution of polyether polyol with soy-based polyol. Eur. Polym. J. 107, 105–117 (2018). https://doi.org/10.1016/j.eurpolymj.2018.08.001

86. Zhang, Q., Lin, X., Chen, W., Zhang, H., Han, D.: Modification of rigid polyurethane foams with the addition of nano-SiO2 or lignocellulosic biomass. Polymers (Basel) (2020). https://doi.org/10.3390/polym12010106

87. Foams, P., Gu, R., Sain, M.M.: Effects of wood fiber and microclay on the performance of soy based effects of wood fiber and microclay on the performance of soy based polyurethane foams. J. Polym. Environ. (2014). https://doi.org/10.1007/s10924-012-0538-y

88. Konar, S., Sain, M.: Preparation and characterization of sustainable polyurethane foams from preparation and characterization of sustainable polyurethane foams from soybean oils. J. Am. Oil Chem. Soc. (2012). https://doi.org/10.1007/s11746-012-2109-8

89. Jarfelt, U., Ramnäs, O.: Thermal conductivity of polyurethane foam - best performance Thermal conductivity of polyurethane foam Best performance. 10th Int. Symp. Dist. Heat. Cool. 12 (2006)

90. Andersons, J., Kirpluks, M., Cabulis, P., Kalnins, K., Cabulis, U.: Bio-based rigid high-density polyurethane foams as a structural thermal break material. Constr. Build. Mater. (2020). https://doi.org/10.1016/j.conbuildmat.2020.120471

91. Mohd Sabee, M.M.S., Itam, Z., Beddu, S., Zahari, N.M., Mohd Kamal, N.L., Mohamad, D., Zulkepli, N.A., Shafiq, M.D., Abdul Hamid, Z.A.: Flame retardant coatings: additives, binders, and fillers. Polymers (Basel) (2022). https://doi.org/10.3390/polym14142911

92. Hung Anh, L.D., Pásztory, Z.: An overview of factors influencing thermal conductivity of building insulation materials. J. Build.

Eng. **44**, 102604 (2021). https://doi.org/10.1016/j.jobe.2021.102604

93. Kuźnia, M., Magiera, A., Zygmunt-Kowalska, B., Kaczorek-Chrobak, K., Pielichowska, K., Szatkowski, P., Benko, A., Ziabka, M., Jerzak, W.: Fly ash as an eco-friendly filler for rigid polyurethane foams modification. Materials (Basel) (2021). https://doi.org/10.3390/ma14216604

94. Hung Anh, L.D., Pásztory, Z.: An overview of factors influencing thermal conductivity of building insulation materials. J. Buil. Eng. (2021). https://doi.org/10.1016/j.jobe.2021.102604

95. Kairytė, A., Kirpluks, M., Ivdre, A., Cabulis, U., Vaitkus, S., Pundienė, I.: Cleaner production of polyurethane foam: replacement of conventional raw materials, assessment of fire resistance and environmental impact. J. Clean. Prod. **183**, 760–771 (2018). https://doi.org/10.1016/j.jclepro.2018.02.164

96. Liu, H., Zhang, B., Han, J.: Improving the flame retardancy and smoke suppression properties of polyurethane foams with SiO2 microcapsule and its flame-retardant mechanism. Polym. Plast. Technol. Eng. **57**, 1139–1149 (2018). https://doi.org/10.1080/03602559.2017.1373398

97. Jiao, C., Zhao, L., Chen, X.: Preparation of modified hollow glass microspheres using Fe2O3 and its flame retardant properties in thermoplastic polyurethane. J. Therm. Anal. Calorim. **127**, 2101–2112 (2017). https://doi.org/10.1007/s10973-016-5831-x

98. Mei, N., Mingshuo, Z., Baoxia, X., Ruihong, Q., Mingqiang, S., Li, Z.: Introducing the Fe2O3 particles into fiber for flame retardancy and smoke suppression. J. Text. Inst. (2022). https://doi.org/10.1080/00405000.2022.2026580